

Spatial and sectoral benefit distribution in water-energy system design

Jose M. Gonzalez^a, James E. Tomlinson^a, Julien J. Harou^{a,f,*}, Eduardo A. Martínez Ceseña^b, Mathaios Panteli^b, Andrea Bottacin-Busolin^a, Anthony Hurford^a, Marcelo A. Olivares^c, Afzal Siddiqui^{d,e}, Tohid Erfani^f, Kenneth M. Strzepek^g, Pierluigi Mancarella^{b,h}, Joseph Mutale^b, Emmanuel Obuobieⁱ, Abdulkarim H. Seid^j, Aung Ze Ya^k

^a Department of Mechanical, Aerospace and Civil Engineering, The University of Manchester, Manchester M13 9PL, UK

^b Department of Electrical & Electronic Engineering, The University of Manchester, Manchester M13 9PL, UK

^c Department of Civil Engineering, University of Chile, Blanco Encalada, 2002 Santiago, Chile

^d Department of Statistical Science, University College London, London WC1E 6BT, UK

^e Department of Computer and Systems Sciences, Stockholm University, Sweden

^f Department of Civil, Environmental and Geomatic Engineering, University College London, London WC1E 6BT, UK

^g Joint Program on the Science and Policy of Global Change, MIT, 77 Massachusetts Ave, E19-429F, Cambridge, MA 02139-4307, USA

^h School of Electrical and Electronic Engineering, The University of Melbourne, Melbourne, Australia

ⁱ Water Research Institute, Council for Scientific and Industrial Research, P.O. Box AH 38, Achimota, Accra, Ghana

^j Water Resources Management, Nile Basin Initiative Secretariat, Entebbe, Uganda

^k Department of Electrical Power Engineering, Yangon Technological University, Insein Township, Yangon, Myanmar

HIGHLIGHTS

- A multi-objective water-energy system design framework under uncertainty is presented.
- Implications of spatial topology and interdependencies in multi-sector systems are explored.
- The approach enables water-energy systems design given complex regional and sectoral trade-offs.

ARTICLE INFO

Keywords:

Water-energy system design
Multi-sector benefit distribution
Multi-objective robust optimisation under uncertainty
Multi-objective evolutionary algorithms

ABSTRACT

The design of water and energy systems has traditionally been done independently or considering simplified interdependencies between the two systems. This potentially misses valuable synergies between them and does not consider in detail the distribution of benefits between different sectors or regions. This paper presents a framework to couple integrated water-power network simulators with multi-objective optimisation under uncertainty to explore the implications of explicitly including spatial topology and interdependencies in the design of multi-sector integrated systems. A synthetic case study that incorporates sectoral dependencies in resource allocation, operation of multi-purpose reservoirs and spatially distributed infrastructure selection in both systems is used. The importance of explicitly modelling the distribution of benefits across different sectors and regions is explored by comparing different spatially aggregated and disaggregated multi-objective optimisation formulations. The results show the disaggregated formulation identifies a diverse set of non-dominated portfolios that enables addressing the spatial and sectoral distribution of benefits, whilst the aggregated formulations arbitrarily induce unintended biases. The proposed disaggregated approach allows for detailed spatial design of interlinked water and energy systems considering their complex regional and sectoral trade-offs. The framework is intended to assist planners in real resource systems where diverse stakeholder groups are mindful of receiving their fair share of development benefits.

1. Introduction

Investments in large water and energy infrastructures, such as dams,

power plants, water transfers and transmission lines, are typically planned without rigorous consideration of the synergies and trade-offs between the two systems and by simplifying their spatial and sectoral

* Corresponding author.

E-mail address: julien.harou@manchester.ac.uk (J.J. Harou).

<https://doi.org/10.1016/j.apenergy.2020.114794>

Received 18 November 2019; Received in revised form 1 March 2020; Accepted 2 March 2020

Available online 18 May 2020

0306-2619/© 2020 The Authors. Published by Elsevier Ltd. This is an open access article under the CC BY license

(<http://creativecommons.org/licenses/by/4.0/>).

interdependencies [1–6]. This is the result of different regulatory frameworks, differences in spatial and temporal scales and the high computational costs of integrated water-energy modelling. However, the independent and spatially simplified planning of water and energy systems may lead to inefficient resource use and arbitrarily allocation of the benefits across the systems, which can exacerbate conflicts between regions and/or sectors, which may be further increased by the uncertainty associated with future energy and water demands and other unknowns like climate change [7–12]. In this context, integrated and multi-objective planning for expansion of spatially distributed water-energy systems under uncertainty can assist stakeholders in understanding interdependencies and trade-offs between both systems, thereby facilitating improved resource planning [11,12].

The area of water-energy infrastructure planning has motivated substantial work over the past decade [see, e.g. 10–12]. However, due to the complexity inherent in jointly planning water-energy systems, different optimisation strategies have been proposed to design and evaluate water and energy systems. For example, existing work has been based on water- or energy-centred models with simplified spatial and temporal representations of the integrated systems. For example, Ackerman and Fisher [13], using a detailed energy-centred model, evaluated how water availability for cooling impacts the planning of conventional power plants in the long term, including water rights as water availability constraints. Macknick and Cohen [14] used the Regional Energy Deployment System model (ReEDS) to evaluate the impact of high solar photovoltaic electricity penetration on the water withdrawals in the United States. The use of water for cooling thermal generators was used as a proxy to assess the impact on water withdrawals, considering that high penetration of solar electricity reduces water use because thermal generation is displaced. The authors provide insight on the use of water at national and regional scales in the United States. However, they used fixed water rights to represent the actual availability of resources through the system, which assumes a static nature of water resources. Escrivá-Bou et al. [15] presented a modelling framework to integrate water, energy and emissions of greenhouse gases. The framework evaluates the operation of a water resources system involving only water-related energy uses using a water-centred model. Nevertheless, the interaction of water-related energy uses (hydropower, pumped storage) with the full energy system (thermal power plants, transmission lines) was not incorporated.

Due to simplified representations in either water- or energy-centred models, other studies have proposed linking specialised water and energy models in an iterative fashion, thereby creating a sequential link between models. For instance, Howells et al. [16] and Mehta and Yates [17] propose an approach that combines the Water Evaluation and Planning (WEAP) model [18] for water resources modelling, and the Long-range Energy Alternatives Planning (LEAP) model [19] for energy systems planning. These two models were used in an iterative fashion to assess the impacts of climate change on the expansion of the integrated water-energy systems of The Republic of Mauritius and California, USA, respectively. Ibanez et al. [20] used iterative integration to couple PLEXOS Simulation Software [21] and RiverWare [22] to model the United States Western Interconnection system and ten large reservoirs on the Columbia River, respectively. They illustrated the value of linking water and energy models to evaluate the integration of renewable energy into power systems. Even though the previous studies can model different sectors in detail and capture joint impacts, as stated by Khan et al. [10], the convergence or optimality of the solutions cannot be guaranteed. The reason being that iterations between models are not necessarily closed, meaning that iteration is largely ‘one-way’ and solutions among the models do not have complete feedback. Moreover, iterative approaches could be computationally expensive because the models were not designed for iterative applications.

Other joint water-energy planning approaches used economic optimisation, thereby reconciling all goals through commensuration, either monetisation or requiring a priori weighted preferences of the

objectives. Khan et al. [23] presented an optimisation model for integrated water-energy systems planning that considered their spatial and temporal interdependencies and objectives related to the costs of planning and operating the integrated system. Although the spatial and temporal representations of both systems is an improvement, the optimisation did not consider the multi-criteria trade-offs between sectors and the spatial elements beyond the economic impacts of the expansion of infrastructure in the system. Finally, Giudici et al. [24] proposed a dynamic multi-objective design and operation of water-energy systems for off-grid islands, and Parkinson et al. [25] a multi-criteria framework for planning water and energy systems at national or regional scales. In those cases, although a multi-objective analysis to explore trade-offs between conflicting objectives was incorporated, an analysis of the impact of spatial interdependencies and benefits distribution amongst the systems was not addressed. Additionally, most water-energy system design studies do not optimise under uncertainty due to the computationally intensive nature of combined water-energy simulation.

The examples above describe different optimisation approaches and frameworks for designing water-energy infrastructure under different levels of system integration. To the extent of the authors’ knowledge, a generalised multi-objective integrated framework to optimise the spatial interdependencies of integrated water-energy design under uncertainty has not yet been published. This work provides the following contributions:

1. A framework linking a generalised integrated water-power network simulator with multi-objective portfolio optimisation under uncertainty.
2. A spatially aggregated optimised design formulation and a regionally disaggregated one.
3. A demonstration of the benefits of explicitly including spatial interdependencies in the design of multi-sector integrated systems on a synthetic but realistic case study.

The multi-objective optimisation models use a meta-heuristic search algorithm to identify portfolios of infrastructure and policy interventions in the system, such as irrigation canals, transmission lines, thermal and hydroelectric plants and multi-purpose reservoirs and their operating rules. Uncertainty related to river inflows and water and energy demands is incorporated into the multi-objective optimisation models through a scenario ensemble, which is a combination of river inflows and water and energy demand scenarios. Robust interventions in the system are evaluated over the scenario ensemble and are subject to the objectives of the optimisation process.

The paper is organised as follows: Section 2 introduces the proposed framework and describes the generalised water-power network simulation. Section 3 describes the case study and presents the multi-objective optimisation formulations used to investigate the added value of spatial multi-sector design. Sections 4 and 5 present and discuss results and Section 6 concludes.

2. Methods

Fig. 1, shows how the integrated water-power network simulator and the multi-objective meta-heuristic search are combined in a 3-step framework where (i) a water-power network simulation model evaluates joint infrastructure and operating rule interventions for each scenario in an ensemble (Ξ) of plausible futures, (ii) a meta-heuristic search algorithm determines updated values of decision variables passed to the water-power network simulation model. Steps (i) and (ii) are repeated until a stopping criterion is met. In step (iii) a spatial and sectoral benefit distribution assessment of the Pareto-optimal intervention portfolios is conducted to determine whether changes to the problem formulation (its simulator, objectives, spatial-temporal aggregation of performance metrics, constraints, uncertainty ensemble) are warranted. Further details about the different steps are presented below.

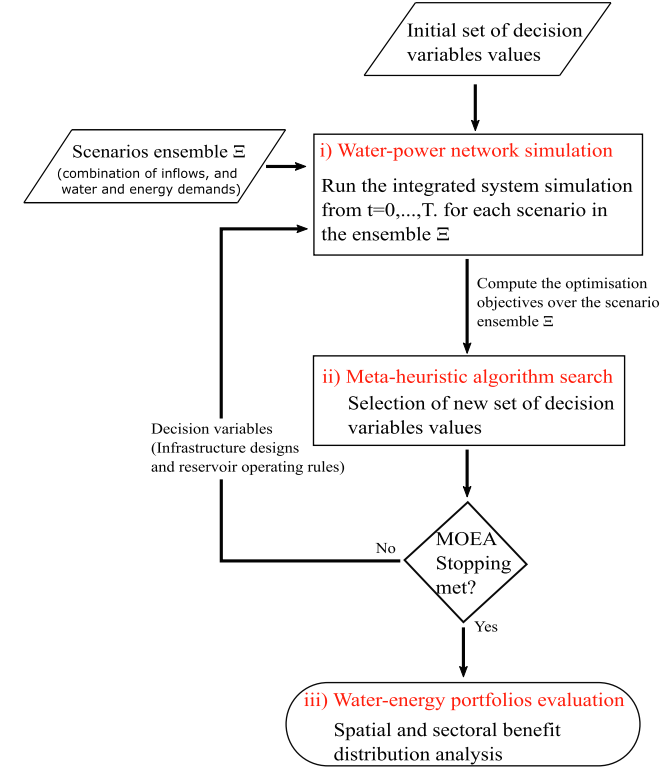


Fig. 1. Illustration of the proposed framework combining integrated water-power network simulators with multi-objective optimisation under uncertainty of spatially and sectorally disaggregated performance metrics.

2.1. Multi-objective optimisation

Multi-objective search problems are those where the goal is to optimise k objective functions simultaneously [26]. The optimisation is defined by the minimisation (or maximisation) of the k functions vector as follows:

$$\min \mathbf{F}(\mathbf{I}) = \{f_1, f_2, f_3, \dots, f_k\} \quad \forall \mathbf{I} \in \Omega \quad (1)$$

Subject to:

$$c_i(\mathbf{I}) = 0 \quad \forall i \in [1, q] \quad (2)$$

$$c_j(\mathbf{I}) \leq 0 \quad \forall j \in [1, r] \quad (3)$$

where \mathbf{I} is a vector of decision variables in the decision space Ω , and the k objective values are evaluated by some function, which in our framework is an external simulator. Depending on the problem there will be q equality (Eq. (2)) and r inequality constraints (Eq. (3)) and feasible solutions are those that meet all the imposed constraints. Finally, the solution to a multi-objective problem in Eq. (1) is the set of non-dominated Pareto-optimal [27] solutions [28].

In the case of water-energy resource systems, planners are typically interested in robust designs, where system performance remains acceptable even if future supply and/or demand are different than originally envisaged. In this case multi-scenario optimisation is warranted, or 'robust optimisation', which is an extension of the optimisation problem formulated in Eqs. (1)–(3). In this case, the robustness is calculated for the decision variable, \mathbf{I} , across a set of future scenarios $S = \{s_1, s_2, \dots, s_n\}$ using the performance metric $f_k(\cdot)$. Whereby, the robustness calculation corresponds to the evaluation of the performance of \mathbf{I} over a set of different scenarios, $\mathbf{F}(\mathbf{I}, S) = \{f_1(\mathbf{I}, S), f_2(\mathbf{I}, S), \dots, f_k(\mathbf{I}, S)\}$ [29]. The way in which system performance (the objective values) is statistically aggregated across the different n scenarios is referred to as a robustness metric. The use of robustness metrics has been recently been reviewed in the literature [29–31].

2.2. Water-power network simulation

The generalised water-power network simulator used here is described by Eqs. (4)–(15). The simulator performs resource allocation throughout the integrated water-power network over a sequence of time steps using linear programming. The objective function minimises the combined costs per time step (t) associated with energy generation (e.g. fuel costs) and the failure to supply water and energy demands.

$$\min_{Gen_{t,en}^g, u_{t,wn}, \vartheta_{t,l}} Z_t = \sum_{en} \sum_g C_g \times Gen_{t,en}^g + \sum_{en} \rho_{en} \times ENS_{t,en} + \sum_{wn} \rho_{wn}^i \times def_{t,wn}^i \quad (4)$$

In Eq. (4), en and wn are the energy and water nodes in the system, g is the set of power generators in the system, including hydropower (hp) and thermal (th) generators; i is the set of water uses, namely irrigation (ir), public water supply (pws) and hydropower (hp); C_g denotes operating costs; $Gen_{t,en}^g$ represents energy generation; $ENS_{t,en}$ represents energy not supplied; and $def_{t,wn}^i$ is the water deficit for each consumptive water use. ρ_{en} and ρ_{wn}^i are the penalties applied for unsupplied energy and water demands, respectively. In practice, these penalties may not represent true financial costs, but must be determined through calibration and validation of the model; in this case, we use the same constant value for both sectors and for all the water uses in the systems. The balance constraints in the network at each wn and en node are given by Eqs. (5) and (6).

$$S_{t+1,wn} = S_{t,wn} + q_{t,wn} + C^R(u_{t,wn}^i - sp_{t,wn}) \quad \forall wn \quad (5)$$

$$\sum_g Gen_{t,en}^g + ENS_{t,en} + \sum_{l:r(l)=en} \vartheta_{t,l} - \sum_{l:s(l)=en} \vartheta_{t,l} = De_{t,en} \quad \forall en \quad (6)$$

In the above equations, $S_{t,wn}$ is the volume of water stored in the multi-purpose reservoir at node wn ; $u_{t,wn}^i$ and $sp_{t,wn}$ represent the water allocation for the water uses in the system and the spill flows from reservoirs, respectively; $q_{t,wn}$ is the inflow; and C^R is the network connectivity matrix in the system [$C_{j,k}^R = 1(-1)$ when the water node $j \in wn$ receives water from (to) water node $k \in wn$]. For releases to consumptive water uses (mainly irrigation uses), the network connectivity matrix can track possible flows that return to the network as a fraction β of the release. In the power network, $\vartheta_{t,l}$ is the electricity transmitted through the transmission line l , which has starting, i.e. $s(l)$, or ending, i.e. $r(l)$, nodes at node en ; and $De_{t,en}$ is the energy demand at en . The maximum water allocation to consumptive uses, the supply of consumptive water demands and the conversion of the turbine flow to energy are constrained by Eqs. (7)–(9), respectively.

$$0 \leq u_{t,wn}^i \leq Ca_{t,wn}^i \quad \forall i = ir, pws, \quad \forall wn \quad (7)$$

$$u_{t,wn}^i = Dw_{t,wn}^i - def_{t,wn}^i \quad \forall i = irr, pws, \quad \forall wn \quad (8)$$

$$Gen_{t,wn \cap en}^g = \eta G \gamma_w \bar{h}_{wn} u_{t,wn \cap en}^i \quad \forall g, \forall i = hp, \quad \forall wn \cap en \quad (9)$$

In the above equations, $wn \cap en$ represents the intersection of nodes connecting the water and the power systems, i.e. hydropower plants. $Ca_{t,wn}^i$ is the canal capacity; $Dw_{t,wn}^i$ is the water demand; η is the turbine efficiency; G is the gravitational acceleration; γ_w is the water density; and \bar{h}_{wn} is the net hydraulic head. Decision variables in the multi-objective optimisation models, target water allocation and maximum infrastructure capacity are linked to the water-power network simulation model according to Eqs. (10)–(14)

$$u_{t,wn}^i \leq I_{t,wn}^i \quad \forall wn, \quad \forall i \in I \quad (10)$$

$$0 \leq Gen_{t,en}^g \leq \bar{P}_{en}^g \quad \forall en, \quad \forall g \in G \quad (11)$$

$$0 \leq \vartheta_{t,l} \leq \bar{\vartheta}_l \quad \forall l \in L \quad (12)$$

$$0 \leq S_{t,wn} \leq \bar{S}_{wn} \quad \forall wn \quad (13)$$

$$Ca_{i,wn}^i = \overline{Ca}_{wn}^i \quad \forall wn, \quad \forall i = ir, wps \quad (14)$$

Note that $r_{i,wn}^i$, P_{en}^g , $\overline{\delta I}_i$, \overline{S}_{wn} and \overline{Ca}_{wn}^i are the decision variables in the multi-objective optimisation models. These variables are taken as fixed parameters by the water-power network simulation model and are updated in each search iteration between both models.

Finally, variables from the water-power network simulation model used to compute the objectives in the multi-objective models (Section 3.2.1) are non-negative real numbers, Eq. (15).

$$\{Gen_{i,en}^h, def_{i,wn}^e, ENS_{i,en}, S_{i,wn}\} \in \mathbb{R}_{\geq 0} \quad \forall en, \quad \forall wn, \quad \forall i \in I, \quad \forall g \in G, \quad \forall t \in T, \quad \forall \Xi \quad (15)$$

3. Investigation

3.1. Case-study

A synthetic case study is used to demonstrate the benefits of spatial multi-sector design (Fig. 2). In this system, water and energy interdependencies related to resource allocation occur via operation of multi-purpose reservoirs. The integrated water-energy system is represented as a network and each node in the network represents a component in the system; these components may be physical infrastructure (such as reservoirs, substations or power plants) or features of the resource system (such as agricultural zones, public water supply and energy demands or catchments). The nodes in the network are linked through canals, rivers or transmission lines.

The integrated water-energy system is divided into two regions, northern and southern, as shown in Fig. 2. This division is used to analyse spatial interdependencies among the different components in the system and their regional implications. The northern region contains irrigation demand 1 (Di1), public water supply-demand 1 (Dp1), energy demand 1 (De1) and the existing and possible new infrastructure (shown in red) used to supply these demands. The southern region contains irrigation demand 2 (Di2), public water supply-demand 2 (Dp2), energy demand 2 (De2) and the associated existing and possible new infrastructure.

Competition exists between the water and the power systems for access to and utilisation of water resources within each region (water

used for irrigation is not available for hydropower generation or public water supply and vice versa). However, all the turbine water of Hp1 is available for any use downstream (i.e., for Dp1 and water uses in the south). In contrast, only 15% of the water utilised in Di1 is available for downstream water uses as irrigation return flow. There is also spatial competition in the use of thermal resources: the energy produced by Th1 (\$43/MWh) in the northern region has lower operating costs than that produced by Th2 (\$214/MWh) in the southern region. The energy produced by the proposed Th3 has an intermediate cost (\$111/MWh) and is located in the northern region. Therefore, although it is preferable to supply energy demand using Th1 and Th3, these can only supply De2 if the transmission line is constructed. The optimisation process identifies promising infrastructure and policy interventions in the system, such as irrigation canals, transmission lines, thermal and hydroelectric plants and multi-purpose reservoirs and their operating rules. Where the operating rules link the intertemporal decisions associated with the reservoir storage in the operation of the integrated system, Table 1 shows the capacity and the annualised investment costs for each option. Annualised investment costs as well as thermal power plant operating costs are taken from the literature [32,33]. These values are realistic for the technologies and infrastructure used in our synthetic case.

Finally, the water-power network simulation model uses monthly time steps (t) over a 50-year time horizon, whence the simulation model runs from $t = 1, \dots, 600$ for each scenario in the ensemble Ξ . In the present study, 20 river inflow scenarios were considered for each water catchment and three scenarios (low, medium and high) for each water and energy demand. The product of all scenarios is an ensemble of 180 scenarios in total.

3.2. Problem formulation

3.2.1. Multi-objective robust optimisation model formulations

Three different formulations of the multi-objective robust optimisation model are implemented (Table 2) to explore the benefits of designing integrated water-energy systems considering sectoral and spatial interdependencies. The robust optimisation [34] considers an ensemble (Ξ) of different water and energy demands and river inflow (supply) scenarios. The robustness of the optimised system design is sought in the search process by considering simulated impacts over all Ξ scenarios aggregated statistically via robustness metrics (Table 2). The optimisation objectives are related to investment and operating costs and to the water and the energy deficit frequencies over the ensemble. Deficit frequencies evaluate the fraction of simulated time-steps where the water and energy supplies are insufficient to meet demands [35].

The above formulations are used to evaluate different representations of the aggregation of the regional water and energy deficit frequency objectives. Two regionally aggregated formulations are implemented using different mathematical operators for aggregation. In the first formulation, the infrastructure and reservoir operating rules are identified by minimising three objectives: (i) mean total system cost; (ii) maximum aggregated water deficit frequency; and (iii) maximum aggregated energy deficit frequency. The second aggregated

Table 1
Feasible infrastructure options.

Options	Option abbreviation	Maximum capacity	Annualised investment costs
Irrigation canal 1	Ca1	5 Mm ³ /day	\$269, 802/Mm ³ day ⁻¹
Thermal plant 3	Th3	3000 MW	\$130, 199/MW
Reservoir 2	S2	1500 Mm ³	\$9, 982/Mm ³
Hydropower plant 2	Hp2	1500 MW	\$90, 380/MW
Transmission line	tl	3000 MW	\$5, 484/MW

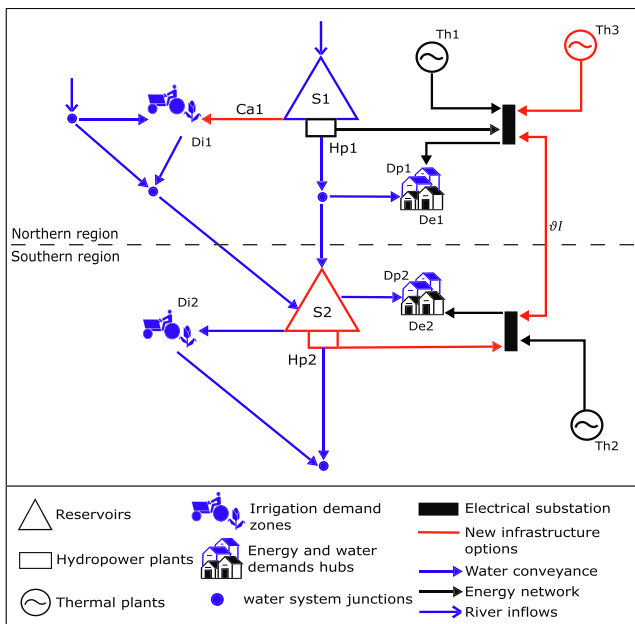


Fig. 2. The water-energy network structure of the synthetic case study. Blue denotes water resource system components, black energy system components, and red shows proposed infrastructure options.

Table 2
Summary of search formulations.

Formulation	Objective function	Robustness metric
Formulation 1	Total system cost	Minimise-Mean
	Aggregated water deficit frequency	Minimise-Maximum
	Aggregated energy deficit frequency	Minimise-Maximum
Formulation 2	Total system cost	Minimise-Mean
	Aggregated water deficit frequency	Minimise-Mean
	Aggregated energy deficit frequency	Minimise-Mean
Formulation 3	Total system cost	Minimise-Mean
	Water deficit frequency in the northern region	Minimise-Maximum
	Water deficit frequency in the southern region	Minimise-Maximum
	Energy deficit frequency in the northern region	Minimise-Maximum
	Energy deficit frequency in the southern region	Minimise-Maximum

formulation minimises: (i) the mean total system cost; ii) the mean aggregated water deficit frequency; and (iii) the mean aggregated energy deficit frequency. Both model formulations are represented by Eqs. (16)–(18).

$$\min_{\Xi} [\text{Total System}_{\text{costs}} = \text{mean}(E_{\text{capex}} + W_{\text{capex}} + \text{Thermal}_{\text{costs}})] \quad (16)$$

$$\min \left[\text{agg. } W_{D_{\text{freq}}} = \theta \max_{\Xi, \text{wn}} \left(\frac{1}{T} \sum_{t=1}^T W_{D_{\text{def}, \text{wn}}} \right) \right] \quad (17)$$

$$\min \left[\text{agg. } E_{D_{\text{freq}}} = \theta \max_{\Xi, \text{en}} \left(\frac{1}{T} \sum_{t=1}^T E_{D_{\text{def}, \text{en}}} \right) \right] \quad (18)$$

where θ is the maximum or the mean operator according to the model formulation (i) regionally maximum-aggregated or (ii) regionally mean-aggregated. $\text{Total System}_{\text{costs}}$ is the total cost of the system; $\text{agg. } W_{D_{\text{freq}}}$ is the aggregated water deficit frequency and $\text{agg. } E_{D_{\text{freq}}}$ is the aggregated energy deficit frequency. The two aggregated deficit frequencies, $\text{agg. } W_{D_{\text{freq}}}$ and $\text{agg. } E_{D_{\text{freq}}}$, are the maximum or mean deficit occurrence for each of the different regionally distributed water and energy uses, respectively. Therefore, we aggregate the objectives over space for each sector using the maximum or the mean operator according to the first or second formulation of the aggregated model, respectively. Additionally, E_{capex} and W_{capex} are the energy and water system capex, respectively; $\text{Thermal}_{\text{costs}}$ is the cost incurred by the use of thermal resources; and $W_{D_{\text{def}, \text{wn}}}$ and $E_{D_{\text{def}, \text{en}}}$ are the deficit occurrence of water and energy per time step and per water node or energy node in the system, respectively. These last two variables take values $\in \{0, 1\}$ that represent the deficit occurrence, with 1 if a deficit exists in any t , or 0 otherwise.

The third model formulation is a regionally disaggregated representation of the system's deficit frequency objectives. Here, the water and energy deficit frequency objectives are not aggregated by region to explore the benefits of designing integrated water-power systems with not reduced spatial aggregation. The infrastructure and reservoir operating rules are selected by minimising five objectives: (i) mean total system cost; (ii) maximum water deficit frequency in the northern region; (iii) maximum energy deficit frequency in the northern region; (iv) maximum water deficit frequency in the southern region; and (v) maximum energy deficit frequency in the southern region, represented by Eqs. (19)–(23).

$$\min_{\Xi} [\text{Total System}_{\text{costs}} = \text{mean}(E_{\text{capex}} + W_{\text{capex}} + \text{Thermal}_{\text{costs}})] \quad (19)$$

$$\min \left[W_{D_{\text{freq}}}^{\text{N}} = \max_{\Xi, \text{wn}} \left(\frac{1}{T} \sum_{t=1}^T W_{D_{\text{def}, \text{wn}}}^{\text{N}} \right) \right] \quad (20)$$

$$\min \left[E_{D_{\text{freq}}}^{\text{N}} = \max_{\Xi} \left(\frac{1}{T} \sum_{t=1}^T E_{D_{\text{def}, \text{en}}}^{\text{N}} \right) \right] \quad (21)$$

$$\min \left[W_{D_{\text{freq}}}^{\text{S}} = \max_{\Xi, \text{wn}} \left(\frac{1}{T} \sum_{t=1}^T W_{D_{\text{def}, \text{wn}}}^{\text{S}} \right) \right] \quad (22)$$

$$\min \left[E_{D_{\text{freq}}}^{\text{S}} = \max_{\Xi} \left(\frac{1}{T} \sum_{t=1}^T E_{D_{\text{def}, \text{en}}}^{\text{S}} \right) \right] \quad (23)$$

$W_{D_{\text{freq}}}^{\text{N}}$ and $E_{D_{\text{freq}}}^{\text{N}}$ are the water and energy deficit frequencies in the northern region, respectively and $W_{D_{\text{freq}}}^{\text{S}}$ and $E_{D_{\text{freq}}}^{\text{S}}$ are the water and energy deficit frequencies in the southern region, respectively. Additionally, $W_{D_{\text{def}, \text{wn}}}^{\text{N}}$, $E_{D_{\text{def}, \text{en}}}^{\text{N}}$, $W_{D_{\text{def}, \text{wn}}}^{\text{S}}$ and $E_{D_{\text{def}, \text{en}}}^{\text{S}}$ are the deficits occurrence of water and energy per time step and per water node or energy node in the northern and southern regions, respectively. The variables in the objectives for the model formulations are represented by Eqs. (24)–(28).

$$E_{\text{capex}} = \sum_{\text{en}} \sum_g aCP_g \times \bar{P}_{\text{en}}^g + \sum_{l \in \text{en}} aC\vartheta I_l \times \bar{\vartheta} I_l \quad (24)$$

$$W_{\text{capex}} = \sum_{\text{wn}} aCS_{\text{wn}} \times \bar{S}_{\text{wn}} + \sum_{\text{wn}} aCCa_{\text{wn}} \times \bar{C}a_{\text{wn}} \quad (25)$$

$$\text{Thermal}_{\text{costs}} = \sum_{t=1}^T \sum_{\text{en}} \sum_{(th) \in g} C_{th} \times \text{Gen}_{t, \text{en}}^{th} \quad (26)$$

$$W_{D_{\text{def}, \text{wn}}} = \begin{cases} 1 & \text{if } \sum_i \text{def}_{t, \text{wn}}^i \neq \sum_i D w_{t, \text{wn}}^i \quad \forall i = ir, pws \\ 0 & \text{if } \sum_i \text{def}_{t, \text{wn}}^i = \sum_i D w_{t, \text{wn}}^i \quad \forall i = ir, pws \end{cases} \quad (27)$$

$$E_{D_{\text{def}, \text{en}}} = \begin{cases} 1 & \text{if } \text{ENS}_{t, \text{en}} \neq D e_{t, \text{en}} \\ 0 & \text{if } \text{ENS}_{t, \text{en}} = D e_{t, \text{en}} \end{cases} \quad (28)$$

In the above equations, aCP_g , $aC\vartheta I_l$, aCS_{wn} and $aCCa_{\text{wn}}$ are the annualised cost parameters of new infrastructure — power plants, transmission lines, multi-purpose reservoirs and water-supply canals, respectively; \bar{P}_{en}^g is the new power plant capacity per power generator in each energy node in the system network; $\bar{\vartheta} I_l$ is the capacity of the new transmission line l in the system; \bar{S}_{wn} is the capacity of the new multi-purpose reservoir per water node in the system network; $\bar{C}a_{\text{wn}}$ is the capacity of the new water supply canal per water node; C_{th} is the operating cost incurred by thermal energy generation; $\text{Gen}_{t, \text{en}}^{th}$ is the thermal energy generation in the system per t and en .

The variables of the multi-objective models are associated with the new infrastructure options and, in the case of multi-purpose reservoirs, their operating rules. It must be noted that these variables are passed to the water-power network simulation model, which is executed to evaluate the objectives. The type of decision variables is given by Eq. (29).

$$\{\bar{P}_{\text{en}}^g, \bar{\vartheta} I_l, \bar{S}_{\text{wn}}, \bar{C}a_{\text{wn}}, \hat{r}_{t, \text{wn}}^i, \hat{S}_{\text{wn}}\} \in \mathbb{R}_{\geq 0} \quad \forall \text{en}, \quad \forall l, \quad \forall \text{wn}, \quad \forall i \in I, \quad \forall t \in T \quad (29)$$

In Eq. (29), $\hat{r}_{t, \text{wn}}^i$ is the target water allocation variables per water use that depend on a storage volume \hat{S}_{wn} threshold in the reservoirs. Eq. (30) presents the reservoir operating rule with the decision variables of the multi-objective models; this operating rule links the intertemporal decisions associated with the reservoir storage in the water-power network simulation model (Section 2.2).

$$r_{t, \text{wn}}^i = \begin{cases} \hat{r}_{t, \text{wn}}^i & \text{if } S_{t, \text{wn}} \geq \hat{S}_{\text{wn}} \\ \hat{r}_{t, \text{wn}}^i & \text{otherwise} \end{cases} \quad \forall \text{wn}, \quad \forall i \in I, \quad \forall t \in T \quad (30)$$

In Eq. (30), $r_{t, \text{wn}}^i$ is the target water allocation to the different water uses, which include ir , pws and hp , and $S_{t, \text{wn}}$ is the volume of water stored in the multi-purpose reservoirs at node wn , which is calculated in the water-power network simulation model (Section 2.2).

3.2.2. Numerical experiments

In this study the multi-objective evolutionary algorithms (MOEA) was selected to conduct the optimisation of the different multi-objective formulations implemented. MOEAs are established iterative population-based meta-heuristic search algorithms used to identify a Pareto-approximate set of solutions, using operations that mimic natural evolutionary processes to explore and exploit the search space [36–38]. These algorithms have been proven effective for planning and operating water and energy systems independently [3,6,39–44]. Unlike traditional mathematical programming approaches, these algorithms are flexible enough to address systems dimensionality, non-linear relationships between variables, parameter uncertainty and links with simulation models [26,36–38]. MOEAs enable water-energy systems design given the non-linear, multi-objective and stochastic nature of such systems.

The Non-dominated Sorted Genetic Algorithm II (NSGA-II) [45] was used here to identify the robust Pareto front. The MOEA is configured to run for 30,000 function evaluations for each of 30 random seeds (i.e. 900,000 simulations for the scenario ensemble Ξ). The random seeds mitigate randomness dependence and improve solution diversity. The final Pareto-optimal policies are obtained as the set of non-dominated solutions from the combined results of all optimisations [46].

4. Results

Results demonstrate the ability of the proposed framework to explore and recommend system-scale infrastructure designs considering sectoral and spatial dependencies. In addition, results help analyse the benefits of explicitly including spatial resources allocation interdependencies in optimised water-energy system design. Fig. 3 shows three parallel axis plots [47] comparing the regional and sectoral water and energy deficit frequencies and total costs of the optimised system designs for the three model formulations. Each line in Fig. 3 represents a non-dominated (Pareto-optimal) portfolio which corresponds to a unique set of new infrastructure and operation of multi-purpose reservoirs. An ideal solution would lead to a straight horizontal line that intersects every axis at the top. Crossing lines between axes indicate trade-offs between the metrics. The complete set of non-dominated portfolios are represented by grey, coloured (green, red and blue) and black lines. The coloured lines highlight portfolios which are ranked in the top 25% for all deficit metrics for the different water and energy users in both regions. The black lines in the 3 panels show the best equitable portfolio, i.e., a portfolio with the minimum relative difference in the deficit frequency metrics between equivalent users amongst the regions (e.g. difference between irrigation deficit frequency Northern region and the Southern region).

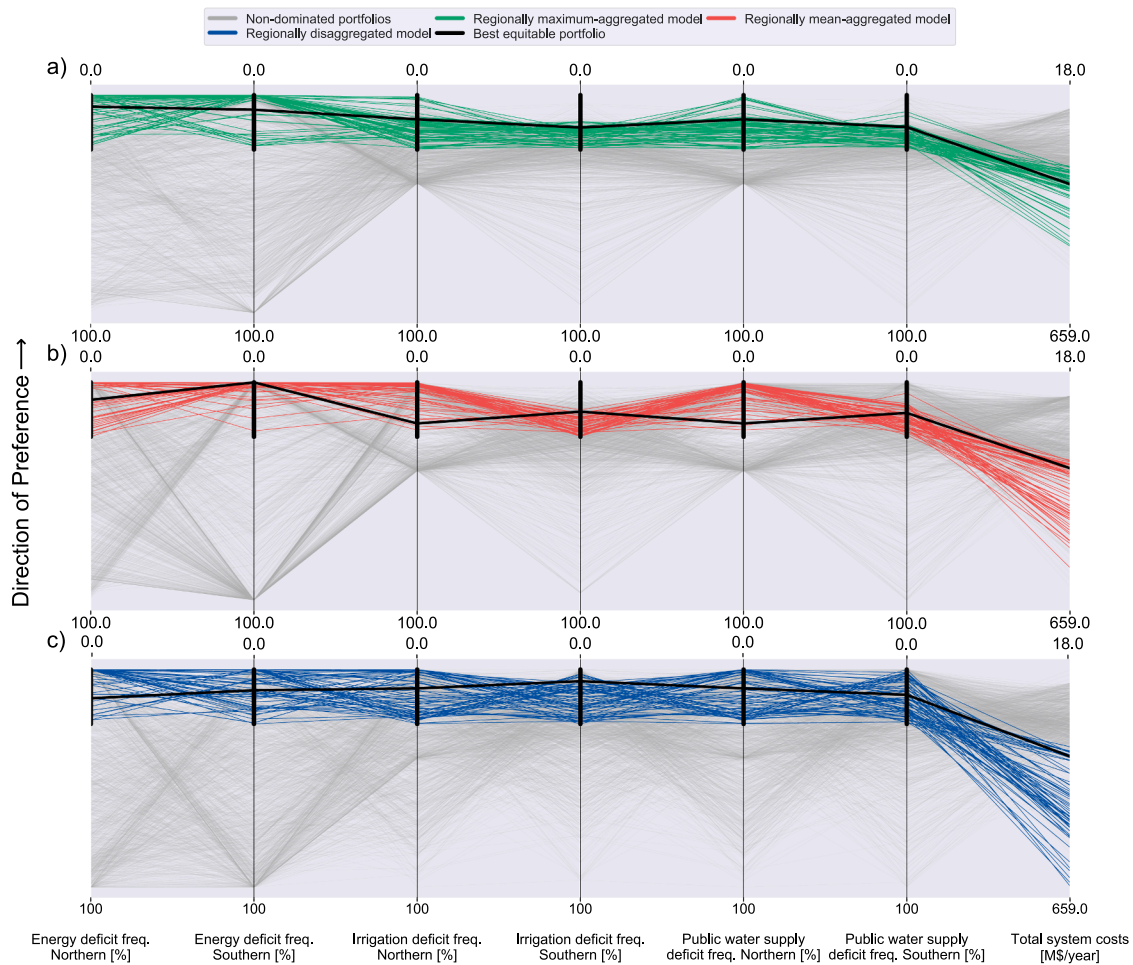


Fig. 3. Parallel axis plot comparing the regional and sectoral water and energy deficit frequencies and the total costs of the system designs of the three model formulations. Panel (a) shows the regionally aggregated model results with the maximum operator, panel (b) the regionally aggregated model results with the mean operator and panel (c) the regionally disaggregated model results. The non-dominated portfolios are filtered to highlight (in colour) those portfolios which have deficit frequencies of less than 25% for the six spatially disaggregated metrics. The figure shows the disaggregated model formulation results covering a larger space of the performance metrics compared to the results of the aggregated formulations. This allows finding a diverse set of non-dominated portfolios that explores all possible trade-offs among the regions and sectors and also finds portfolios that equitably distribute the resources (black line in panel c) without deteriorating overall performance (black line in panel c is closer to the top than in panels a and b).

Table 3
Statistical summary of the results.

Metrics	Maximum-aggregated			Mean-aggregated			Disaggregated		
	Max	Min	σ	Max	Min	σ	Max	Min	σ
Irrigation deficit freq. South [%]	25	8.9	3.1	25	9.5	3.6	25	0	6.4
Irrigation deficit freq. North [%]	25	0.1	6.3	24.6	0	5.7	25	0	8.3
Public water supply deficit freq. South [%]	25	4.3	3.2	25	3.9	5.2	25	0	6.3
Public water supply deficit freq. North [%]	25	0.1	6.3	24.6	0	5.7	25	0	8.3
Energy deficit freq. South [%]	25	0	7.1	24.9	0	5.7	25	0	7.5
Energy deficit freq. North [%]	25	0	7.9	25	0	7.5	25	0	7.8

Panels 3a and 3b show the non-dominated portfolios selected by the maximum- and mean-aggregated model formulations, respectively. It can be seen in these panels that the full extent of the water deficits frequency metrics in the northern region are not explored and water distribution is biased to the water users in this region (i.e., there are no Pareto-optimal solutions where the northern region has low agricultural and municipal water deliveries). Also, there is no Pareto-optimal solution that achieves better than a 13% water deficit metrics in the southern region (see green and red lines). In contrast, solutions with 0% water deficit frequency are available in the northern region. This regional bias in the resource allocation in the aggregated formulations occurs because the search algorithm has no incentive to explore the full objective space and find portfolios that share resources acceptably amongst the regions; it does not look beyond aggregated performance. Note that a rigorous search of the objective space was conducted; we compute the hypervolume [48] for the 30 random seeds and, in general,

for the three formulations, the hypervolume is stabilised in 20,000 function evaluations of the 30,000 evaluations used (see Appendix A).

Conversely, Panel 3c shows that the Pareto-optimal portfolios found by the disaggregated model formulation cover a greater range of the performance space compared to the results of the aggregated models in Panels 3a–3b. This is true for the highlighted top 25% performers (see the standard deviation in Table 3; the higher the standard deviation the higher the variability of the portfolios), but also for the rest of the Pareto space covered by the grey portfolio lines. The explicit incorporation of regional objectives drives the search algorithm to find Pareto-optimal solutions that explore the full distribution of water-energy benefits for the two regions. For instance, in addition to exploring and finding diverse portfolios, the disaggregated formulation found portfolios that relatively equitably distribute resources amongst the regions and the sectors in the system (e.g. black line) and do not deteriorate the overall deficit performance in the system beyond 25%

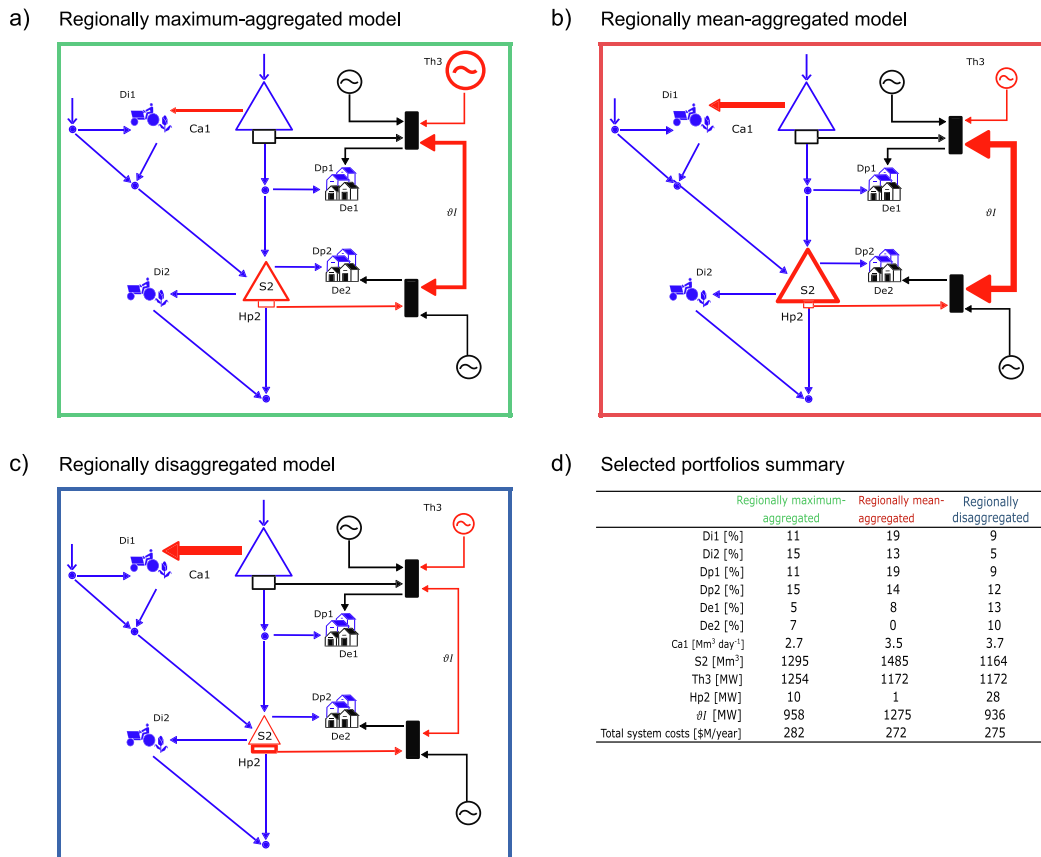


Fig. 4. Spatial distribution of the optimised water-energy infrastructure portfolios and a summary table of system performance for the equitable portfolios highlighted with black lines in Fig. 3. Panel (a)–(c) show the equitable portfolios for the regionally maximum-aggregated, mean-aggregated and disaggregated model, respectively. New infrastructure is red, and sizes/widths of nodes/links are proportional to the scale of the proposed new asset. Panel (d) shows a summary of the investment and performance magnitude in each portfolio. The figure highlights how the approach allows for detailed spatial design of interlinked water and energy systems which considers their complex regional and sectoral trade-offs.

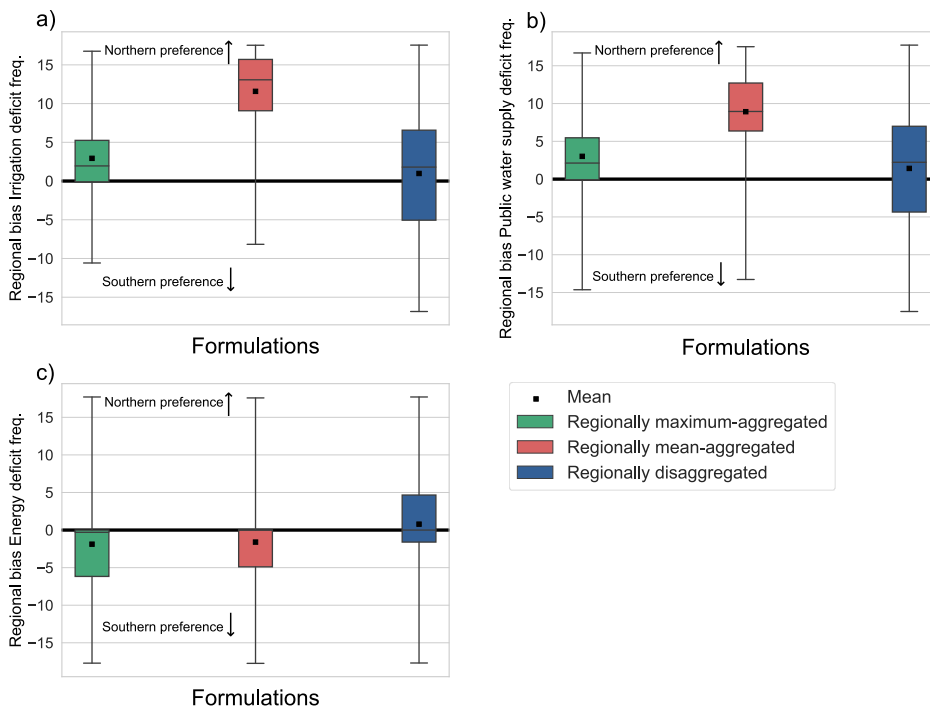


Fig. 5. Regional bias among the water and energy deficit frequencies metrics. Panel (a) show the bias in the Irrigation deficit frequency metrics, (b) bias in the Public water supply deficit frequency metrics and (c) bias in the Energy deficit frequency metrics. Values near zero represent equitable model solutions. Positive values (i.e., top of the plots) indicate a bias to the water and energy users in the northern region and negative values a bias to those in the southern region. The figure shows that arbitrarily unintended biases in the distribution of regional benefits can appear if the spatial nature of the water-energy system is not explicitly considered in the optimised design formulation.

(coloured portfolios). The 3% of the Pareto-optimal portfolios found by the disaggregated formulation, from the blue highlighted portfolios, explore low water deficits in the southern region while the aggregated formulations do not.

Fig. 4, displaying the spatial distribution of the equitable portfolios highlighted with black lines in Fig. 3, shows how the approach allows for detailed spatial design of multi-sector integrated systems. The minimum difference in the evaluated metrics in each highlighted portfolio is 4%, 8% and 4% for the maximum-aggregated, mean-aggregated and disaggregated formulation, respectively. Fig. 4 shows the disaggregated formulation finds solutions that equitably distribute resources without deteriorating overall performance. Conversely, equitable portfolios for the aggregated formulations showed a deterioration in the performance of the southern region, as discussed above.

Next Fig. 5 shows the distribution of a measure of regional bias induced by the different formulations. This measure is estimated by the distance between the equivalent deficit metrics of the users amongst the regions (e.g. Irrigation deficit frequency Northern region vs the Southern region) to a hypothetical equitable solution. This regional bias calculation is described in Appendix B. The bias is calculated using the filtered (coloured lines in Fig. 3) solutions of each model formulation. In Fig. 5, values near zero indicate a regionally equitable distribution, positive values indicate a bias to the water and energy users in the northern region and negative values a southern bias. Panels 5a and 5b show a regional bias that favours water users in the north with the aggregated model formulations. Seventy-five per cent of the northern region water deficit frequencies in the aggregated models are above zero, compared with twenty-five per cent in the South.

There are pronounced differences between the results of the two different aggregated model formulations presented in Panels 5a and 5b. The aggregated model that uses the maximum operator finds portfolios with less regional bias than the mean operator. This is because the maximum operator minimises the worst water deficit frequency

between the water users in the system, which orients the search algorithm to find system configurations that reduce the deficit frequency of the Southern water users compared to the mean aggregation that takes the average deficit frequency. In Panel 5c a similar bias in the aggregated models is evident in the energy sector, however, the bias, in this case, favours southern energy users. The bias in energy sector benefit distribution is not as pronounced as in the water sector because with the construction of the transmission line the electricity can flow towards both regions which gives more flexibility to the power system to allocate the resources amongst the regions.

5. Discussion

In this study, we use different regionally aggregated and disaggregated multi-objective optimisation model formulations to explore the benefits of explicitly including spatial interdependencies in the design of integrated water-energy systems. Results show the disaggregated formulation explores the full extent of the water and energy frequency deficit metrics space, identifying a diverse set of non-dominated portfolios that explore the trade-offs among the regions and the sectors and also finds portfolios that equitably distribute the resources without deteriorating the overall performance of the combined resource system. This diverse range of solutions enables the disaggregated system design formulation to address the distribution of the regional and sectoral benefits explicitly, identifying portfolios that distribute resources to different extents in each region and sector of the system. We found aggregated design formulations showed differing levels of arbitrary biases in the spatial distribution of benefits. We hypothesize that an appropriately equitable set of non-dominated portfolios can help the negotiation of integrated water-energy system designs. It may be appropriate in some cases for one region to obtain a larger share of benefits (e.g. because they are paying more into joint schemes, or because other non-modelled resources are being exchanged between the

countries or regions), so whilst solutions which allocate more to one region are not necessarily bad, an optimised design process should not lead to arbitrary biases in benefit distribution.

Generally, we propose that spatially explicit multi-criteria optimised water-energy system designs can assist planners in complex resources systems where diverse stakeholders groups are intent on receiving a fair share of development benefits. In addition, our results highlight the importance of evaluating the initial conception of the planners' problem formulation to improve its understanding of the problem rather than just providing a single definitive answer to an *a priori* formulation [49].

We use a synthetic case-study to introduce the integrated framework and show the limitations of aggregating by regions and/or sectors in the optimised design of integrated water-energy systems. In real-world design problems involving multiple regions, sectors and objectives, computational limitations of available search algorithms will limit how many objectives can be included. These limitations relate to the use of MOEAs in high-dimensional problems and visualising large data sets and model implementation [50–52]. Despite advances in modern MOEAs, theoretical conditions required for proofs of convergence and solution diversity maintenance remain hard to satisfy in high-dimensional problems [37,44]. In future work one could try reducing the problem dimensionality of disaggregated objectives. Might it be possible to have an aggregated objective that represents the magnitude of an aggregated benefit over all regions and another one preventing their excessively unequitable distribution between regions? Could this help control the number of objectives? This question is left to future work.

6. Conclusions

This paper describes a framework that explicitly considers spatial interdependencies and the spatial distribution of benefits in the design of multi-sector integrated regional resource systems. The proposed framework can support water-energy system planners in multi-sector regional infrastructure design under uncertainty. A synthetic case study solves a proof-of-concept portfolio design problem demonstrating the applicability of the framework. The multi-objective optimisation identifies efficient portfolios of infrastructure and policy interventions in the combined system which includes irrigation canals, transmission lines, thermal and hydroelectric plants, multi-purpose reservoirs and their operating rules. Different formulations of a multi-objective optimisation were implemented incorporating different representations of the aggregation of the sectoral and regional objectives of the system. Using different model formulations, we explored the implications of optimising water-energy infrastructure portfolios based on the distributions of their sectoral and regional benefits. The work highlights the importance, previously noted by other authors cited above, of posing and evaluating different versions of the optimisation problem formulation to improve understanding of the problem rather than just using a single *a priori* defined formulation.

Results showed that the disaggregated model formulation more fully explored the water and energy frequency deficit metric spaces, identifying a diverse set of possible non-dominated portfolios that seek the most efficient trade-offs amongst the regions and the sectors. It also finds portfolios that distribute the benefits equitably without deteriorating overall performance. In our test case the aggregated formulations arbitrarily induced unintended biases in the regional distribution of benefits; with different search objective aggregations producing differing biases.

This paper aims to demonstrate to policy-makers the importance of spatial interdependencies when seeking regionally and sectorally equitable water-energy system designs. The proposed spatial water-energy design approach can assist planners of complex resource systems where different stakeholder groups are intent on obtaining a fair share of development benefits.

Nomenclature

Indices

T	index for time, $t \in \{1, 2, \dots, T\}$
hp	index for hydropower plants
th	index for conventional power plants
l	index for new transmission lines
ir	index for irrigation users
pws	index for public water supply users
N	index for Northern region
S	index for Southern region

Sets

en	set of energy nodes in the system
g	set of power plants in the system
wn	set of water nodes in the system
i	set of water users in the system

Parameters

$De_{t,en}$	energy consumption in en [MWh]
$Dw_{t,wn}^i$	water consumption in wn by each i [Mm^3/day]
η	turbine efficiency [%]
G	gravitational acceleration [m/s^2]
γ_w	water density [kg/m^3]
β	irrigation flows return fraction

Variables

$Gen_{t,en}^g$	energy generation [Mwh]
$ENS_{t,en}$	energy not supplied [Mwh]
$def_{t,wn}^i$	water deficit [Mm^3/day]
$S_{t,wn}$	reservoir storage [Mm^3]
$q_{t,wn}$	reservoir inflows [Mm^3/day]
\bar{P}_{en}^g	power plant maximum capacity [Mw]
$u_{t,wn}^i$	reservoir releases [Mm^3/day]
$sp_{t,wn}$	reservoir spill [Mm^3/day]
$\mathcal{E}_{t,l}$	energy transmitted through transmission line [Mwh]
$Ca_{t,wn}^i$	water canal capacity [Mm^3/day]
\bar{h}_{wn}	water elevation [m]
$r_{t,wn}^i$	reservoir target release [Mm^3/day]
$\bar{Ca}_{t,wn}^i$	water canal maximum capacity [Mm^3/day]
$\bar{\mathcal{E}}_l$	transmission line maximum capacity [Mw]
\bar{S}_{wn}	reservoir maximum capacity [Mm^3]

Indicators

\mathcal{E}	stream flows ensemble
C_g	operating costs [$\$/MWh$]
ρ_{en}	unsupplied energy demand penalty [$\$/MWh$]
ρ_{wn}^i	unsupplied water demand penalty [$\$/Mm^3 \text{ day}^{-1}$]
Total system _{costs}	Total system costs [$\$$]
E_{capex}	capex energy system [$\$$]
W_{capex}	capex water system [$\$$]
Thermal _{costs}	operational thermal costs [$\$$]
agg. W_{Dfreq}	water deficit frequency [%]

$agg. E_{D_{freq}}$	energy deficit frequency [%]
aCP_g	annualised power plant cost [\$/MW]
$aC\vartheta_l$	annualised transmission line costs [\$/MW]
aCS_{wn}	annualised reservoirs costs [\$/Mm ³]
CCa_{wn}	annualised canals costs [\$/Mm ³ day ⁻¹]

CRedit authorship contribution statement

Jose M. Gonzalez: Conceptualization, Methodology, Software, Formal analysis, Writing - original draft, Visualization. **James E. Tomlinson:** Conceptualization, Methodology, Software, Formal analysis, Writing - review & editing. **Julien J. Harou:** Conceptualization, Supervision, Writing - review & editing. **Eduardo A. Martínez Ceseña:** Conceptualization, Methodology, Writing - review & editing. **Mathaios Panteli:** Conceptualization, Writing - review & editing. **Andrea Bottacin-Busolin:** Conceptualization, Writing - review & editing. **Anthony Hurford:** Conceptualization, Writing - review & editing. **Marcelo A. Olivares:** Conceptualization, Writing - review & editing. **Afzal Siddiqui:** Conceptualization, Writing - review & editing. **Tohid Erfani:** Conceptualization, Writing - review & editing. **Kenneth M. Strzepek:** Conceptualization, Writing - review & editing. **Pierluigi Mancarella:** Conceptualization, Writing - review & editing. **Joseph**

Appendix A. Algorithm search convergence

The algorithm search for each model formulation was configured to run for 30,000 function evaluations for each of 30 randomly generated seeds. The use of random seeds mitigates randomness dependence and improves solution diversity. Moreover, it allows to perform a sensitivity analysis of the optimisation process. In Figure A1, we show the evolution of hypervolume [48] for the 30 random seeds. This figure shows that, in general, for the three formulations, the hypervolume is stabilised in ~20,000 function evaluations of the 30,000 evaluations used in each run.

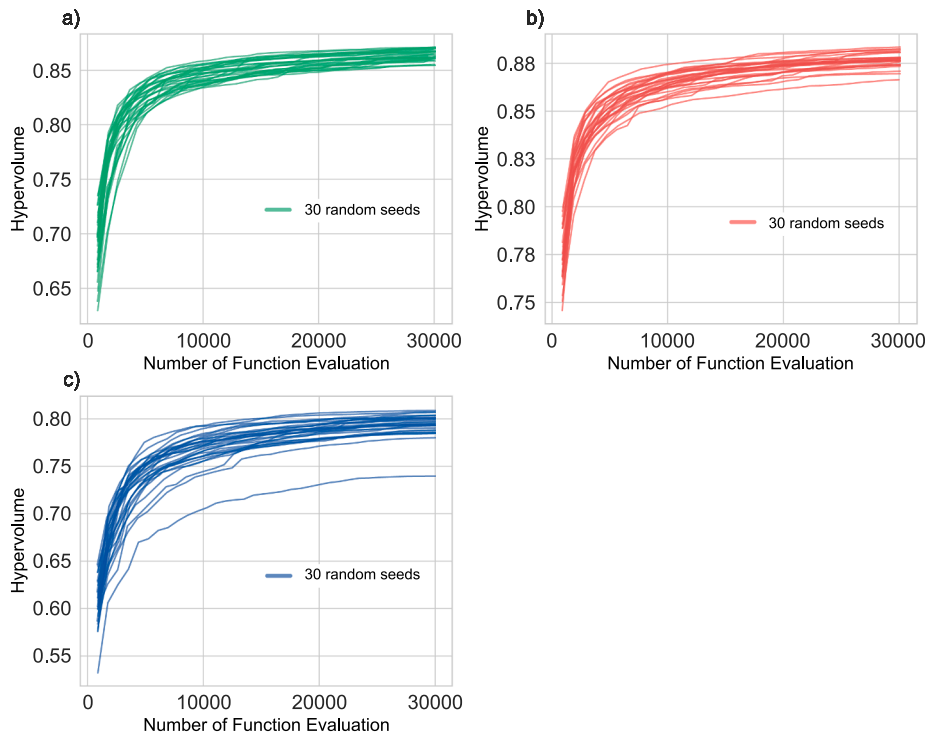


Fig. A1. Hypervolume resulted from the algorithm search by each randomly generated seed. Each line represents the hypervolume attained as a function of the number of function evaluation by each random seed.

Mutale: Conceptualization, Writing - review & editing. **Emmanuel Obuobie:** Conceptualization, Writing - review & editing. **Abdulkarim H. Seid:** Conceptualization, Writing - review & editing. **Aung Ze Ya:** Conceptualization, Writing - review & editing.

Declaration of Competing Interest

The authors declare that they have no known competing financial interests or personal relationships that could have appeared to influence the work reported in this paper.

Acknowledgements

The authors acknowledge UKRI research funding through the “Future Design and Assessment of water-energy-food-environment Mega Systems” (FutureDAMS) research project (ES/P011373/1).

Data availability

The synthetic case study and the data could be found in the repository: <https://github.com/UMWRG/hydraville>.

Appendix B. Regional bias calculation method

The regional bias is calculated by the distance between the equivalent deficit metrics of the users amongst the regions (e.g. Irrigation deficit frequency Northern region vs the Southern region) to a hypothetical equitable solution. The bias is calculated using the coloured solutions of each model formulation. To define the solution of equity, we plotted in a scatterplot each pair of equivalent water and energy metric (Fig. A2) and we defined a 1:1 diagonal line to represent equitable solutions between the metrics evaluated. Next, we calculated the perpendicular distance of each point to the equity line.

Each point in Fig. A2 represents a water or energy deficit frequency associated with a Pareto-optimal portfolio. Solutions in the upper-left have lower deficit frequencies in the northern region, and solutions in the lower-right have lower deficit frequencies in the southern region. The distance of each optimised non-dominated portfolio to the equity line is calculated as shown in Fig. A3.

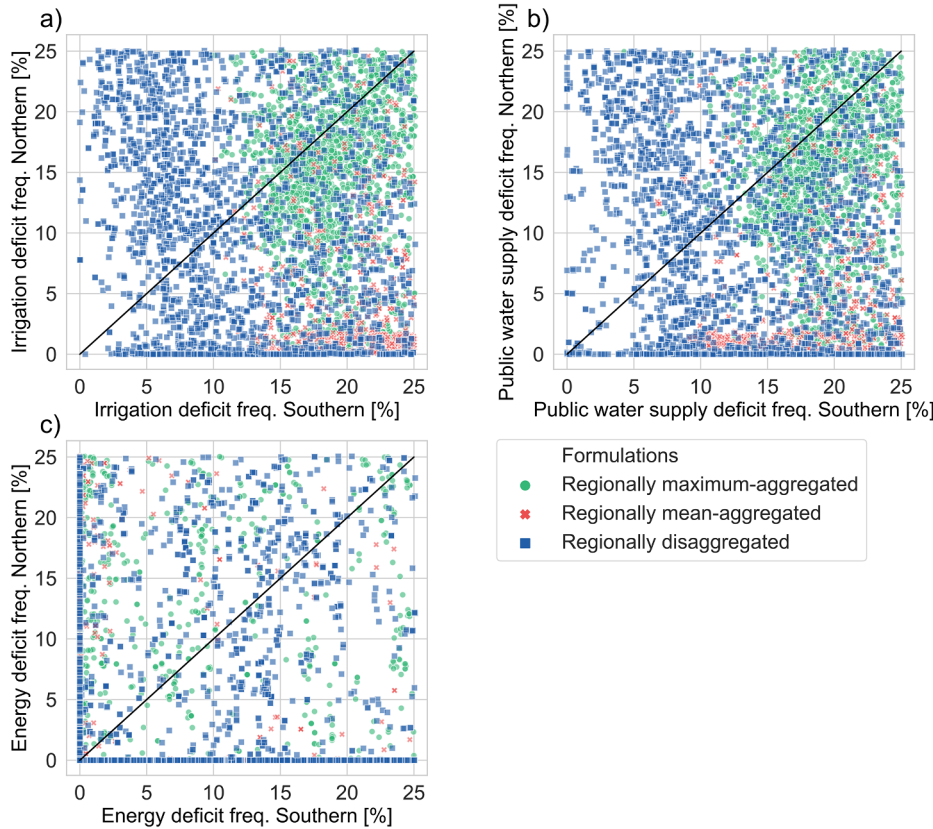


Fig. A2. Scatterplot showing the regional benefits distribution bias, resulting from the optimised infrastructure designs. Panel (a) shows the pair of irrigation deficit frequencies metrics, panel (b) the pair of public water supply deficit frequencies and panel (c) the pair of energy deficit frequencies for the southern and northern regions, respectively. Each point in the figure represents a water or energy deficit frequency associated with a Pareto-optimal portfolio selected by the models. The diagonal black line indicates equally distributed regional performance.

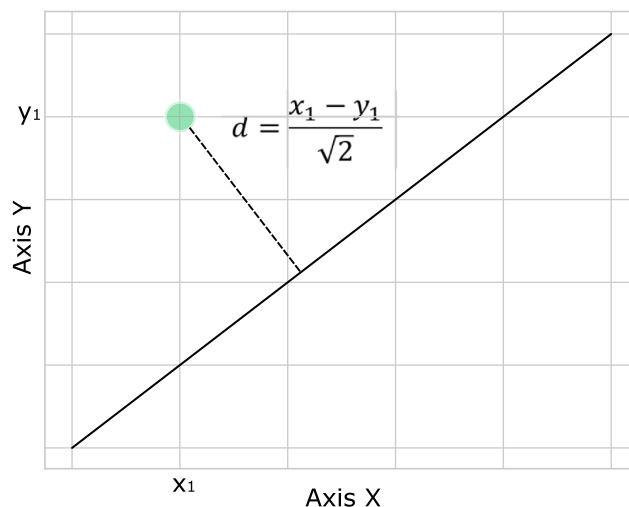


Fig. A3. Method to calculate the perpendicular distance of each point in Fig. A2 to the equity line. This distance is used to measure bias in regional distribution of benefits.

Appendix C. Supplementary material

Supplementary data to this article can be found online at <https://doi.org/10.1016/j.apenergy.2020.114794>.

References

- [1] Loucks DP. Water resource systems models: their role in planning. *J Water Resour Plan Manag* 1992;118:214–23. [https://doi.org/10.1061/\(ASCE\)0733-9496\(1992\)118:3\(214\)](https://doi.org/10.1061/(ASCE)0733-9496(1992)118:3(214)).
- [2] Miloradov M. Planning and management of water-resource systems in developing countries. *J Water Resour Plan Manag* 1992;118:603–19. [https://doi.org/10.1061/\(ASCE\)0733-9496\(1992\)118:6\(603\)](https://doi.org/10.1061/(ASCE)0733-9496(1992)118:6(603)).
- [3] Murugan P, Kannan S, Baskar S. NSGA-II algorithm for multi-objective generation expansion planning problem. *Electr Power Syst Res* 2009;79:622–8. <https://doi.org/10.1016/j.epsr.2008.09.011>.
- [4] Miao DY, Li YP, Huang GH, Yang ZF, Li CH. Optimization model for planning regional water resource systems under uncertainty. *J Water Resour Plan Manag* 2014;140:238–49. [https://doi.org/10.1061/\(ASCE\)WR.1943-5452.0000303](https://doi.org/10.1061/(ASCE)WR.1943-5452.0000303).
- [5] Sadeghi H, Rashidinejad M, Abdollahi A. A comprehensive sequential review study through the generation expansion planning. *Renew Sustain Energy Rev* 2017;67:1672–82. <https://doi.org/10.1016/j.rser.2016.09.046>.
- [6] Wild TB, Reed PM, Loucks DP, Mallen-Cooper M, Jensen ED. Balancing hydropower development and ecological impacts in the mekong: tradeoffs for Sambor mega dam. *J Water Resour Plan Manag* 2019;145:05018019. [https://doi.org/10.1061/\(ASCE\)WR.1943-5452.0001036](https://doi.org/10.1061/(ASCE)WR.1943-5452.0001036).
- [7] Hamiche AM, Stambouli AB, Flazi S. A review of the water-energy nexus. *Renew Sustain Energy Rev* 2016;65:319–31. <https://doi.org/10.1016/j.rser.2016.07.020>.
- [8] Smajgl A, Ward J, Pluschke L. The water-food-energy Nexus – realising a new paradigm. *J Hydrol* 2016;533:533–40. <https://doi.org/10.1016/j.jhydrol.2015.12.033>.
- [9] Al-Saidi M, Elagib NA. Towards understanding the integrative approach of the water, energy and food nexus. *Sci Total Environ* 2017;574:1131–9. <https://doi.org/10.1016/j.scitotenv.2016.09.046>.
- [10] Khan Z, Linares P, García-González J. Integrating water and energy models for policy driven applications. A review of contemporary work and recommendations for future developments. *Renew Sustain Energy Rev* 2017;67:1123–38. <https://doi.org/10.1016/j.rser.2016.08.043>.
- [11] Dai J, Wu S, Han G, Weinberg J, Xie X, Wu X, et al. Water-energy nexus: a review of methods and tools for macro-assessment. *Appl Energy* 2018;210:393–408. <https://doi.org/10.1016/j.apenergy.2017.08.243>.
- [12] Vakilifard N, Anda M, Bahri PA, Ho G. The role of water-energy nexus in optimising water supply systems – Review of techniques and approaches. *Renew Sustain Energy Rev* 2018;82:1424–32. <https://doi.org/10.1016/j.rser.2017.05.125>.
- [13] Ackerman F, Fisher J. Is there a water-energy nexus in electricity generation? Long-term scenarios for the western United States. *Energy Policy* 2013;59:235–41. <https://doi.org/10.1016/j.enpol.2013.03.027>.
- [14] Macknick J, Cohen S. Water impacts of high solar PV electricity penetration. *National Renewable Energy Laboratory, NREL*; 2007.
- [15] Escrivá-Bou A, Lund JR, Pulido-Velazquez M, Hui R, Medellín-Azuara J. Developing a water-energy-GHG emissions modeling framework: Insights from an application to California's water system. *Environ Model Softw* 2018;109:54–65. <https://doi.org/10.1016/j.envsoft.2018.07.011>.
- [16] Howells M, Hermann S, Welsch M, Bazilian M, Segerström R, Alfstad T, et al. Integrated analysis of climate change, land-use, energy and water strategies. *Nat Clim Chang* 2013;3:621–6. <https://doi.org/10.1038/nclimate1789>.
- [17] Mehta V, Yates D. Integrated water-energy-emissions analysis: applying LEAP and WEAP together in California. *Stock Environ Inst Policy Br* 2012.
- [18] Kirshen P, Raskin P, Hansen E. WEAP: a tool for sustainable water resources planning in the border region. *Proc 22nd annu water resour plan manag div conf ASCE integr water resour plan 21st century*. 1995.
- [19] Heaps CG. Long-range Energy Alternatives Planning (LEAP) system [Software version: 2018.1.23]. Somerville (MA, USA): Stockholm Environment Institute; 2016. <https://www.energycommunity.org>.
- [20] Ibanez E, Magee T, Clement M, Brinkman G, Milligan M, Zagona E. Enhancing hydropower modeling in variable generation integration studies. *Energy* 2014;74:518–28. <https://doi.org/10.1016/j.energy.2014.07.017>.
- [21] Energy Exemplar PLEXOS; 2020. <http://energyexemplar.com/software/> [accessed January 27, 2020].
- [22] Zagona E. RiverWare; 2013. www.riverware.org [accessed January 27, 2020].
- [23] Khan Z, Linares P, Rutten N, Parkinson S, Johnson N, García-González J. Spatial and temporal synchronization of water and energy systems: towards a single integrated optimization model for long-term resource planning. *Appl Energy* 2018;210:499–517. <https://doi.org/10.1016/j.apenergy.2017.05.003>.
- [24] Giudici F, Castelletti A, Garofalo E, Giuliani M, Maier HR. Dynamic, multi-objective optimal design and operation of water-energy systems for small, off-grid islands. *Appl Energy* 2019;250:605–16. <https://doi.org/10.1016/j.apenergy.2019.05.084>.
- [25] Parkinson SC, Makowski M, Krey V, Sedraoui K, Almasoud AH, Djilali N. A multi-criteria model analysis framework for assessing integrated water-energy system transformation pathways. *Appl Energy* 2018;210:477–86. <https://doi.org/10.1016/j.apenergy.2016.12.142>.
- [26] Coello Coello CA, Lamont GB, Van Veldhuizen DA. Evolutionary algorithms for solving multi-objective problems vol. 2. Boston (MA): Springer US; 2007. <https://doi.org/10.1007/978-0-387-36797-2>.
- [27] Pareto V. *Cours D'Economie Politique vols. 1 an.* Lausanne: Rouge; 1896.
- [28] Kasprzyk JR, Nataraj S, Reed PM, Lempert RJ. Many objective robust decision making for complex environmental systems undergoing change. *Environ Model Softw* 2013;42:55–71. <https://doi.org/10.1016/j.envsoft.2012.12.007>.
- [29] McPhail C, Maier HR, Kwakkel JH, Giuliani M, Castelletti A, Westra S. Robustness metrics: how are they calculated, when should they be used and why do they give different results? *Earth's Futur* 2018;6:169–91. <https://doi.org/10.1002/2017EF000649>.
- [30] Herman JD, Reed PM, Zeff HB, Characklis GW. How should robustness be defined for water systems planning under change? *J Water Resour Plan Manag* 2015;141:04015012. [https://doi.org/10.1061/\(ASCE\)WR.1943-5452.0000509](https://doi.org/10.1061/(ASCE)WR.1943-5452.0000509).
- [31] Kwakkel JH, Eker S, Pruyt E. How robust is a robust policy? Comparing alternative robustness metrics for robust decision-making vol. 241. Cham: Springer International Publishing; 2016. <https://doi.org/10.1007/978-3-319-33121-8>.
- [32] Inzunza A, Moreno R, Bernales A, Rudnick H. CVaR constrained planning of renewable generation with consideration of system inertial response, reserve services and demand participation. *Energy Econ* 2016;59:104–17. <https://doi.org/10.1016/j.eneco.2016.07.020>.
- [33] Volta River Authority. Institutional, social and economic study for the development of 20 000 ha irrigated scheme as part of the Pwalugu Multipurpose Project; 2019.
- [34] Deb K, Gupta H. Introducing robustness in multi-objective optimization. *Evol Comput* 2006;14:463–94. <https://doi.org/10.1162/evco.2006.14.4.463>.
- [35] Sandoval-Solis S, McKinney DC, Loucks DP. Sustainability index for water resources planning and management. *J Water Resour Plan Manag* 2011;137:381–90. [https://doi.org/10.1061/\(ASCE\)WR.1943-5452.0000134](https://doi.org/10.1061/(ASCE)WR.1943-5452.0000134).
- [36] Nicklow J, Reed P, Savic D, Dessalegne T, Harrell L, Chan-Hilton A, et al. State of the art for genetic algorithms and beyond in water resources planning and management. *J Water Resour Plan Manag* 2010;136:412–32. [https://doi.org/10.1061/\(ASCE\)WR.1943-5452.0000053](https://doi.org/10.1061/(ASCE)WR.1943-5452.0000053).
- [37] Maier HR, Kapelan Z, Kasprzyk J, Kollat J, Matott LS, Cunha MC, et al. Evolutionary algorithms and other metaheuristics in water resources: Current status, research challenges and future directions. *Environ Model Softw* 2014;62:271–99. <https://doi.org/10.1016/j.envsoft.2014.09.013>.
- [38] Maier HR, Razavi S, Kapelan Z, Matott LS, Kasprzyk J, Tolson BA. Introductory overview: optimization using evolutionary algorithms and other metaheuristics. *Environ Model Softw* 2018. <https://doi.org/10.1016/j.envsoft.2018.11.018>.
- [39] Kollat JB, Reed PM. A computational scaling analysis of multiobjective evolutionary algorithms in long-term groundwater monitoring applications. *Adv Water Resour* 2007;30:408–19. <https://doi.org/10.1016/j.advwatres.2006.05.009>.
- [40] Sirikum J, Techanitawad A, Kachitvichyanukul V. A new efficient GA-benders' decomposition method: for power generation expansion. *IEEE Trans Power Syst* 2007;22:1092–100.
- [41] Kannan S, Baskar S, McCalley JD, Murugan P. Application of NSGA-II algorithm to generation expansion planning. *IEEE Trans Power Syst* 2009;24:454–61. <https://doi.org/10.1109/TPWRS.2008.2004737>.
- [42] Fernandez AR, Blumsack SA, Reed PM. Operational constraints and hydrologic variability limit hydropower in supporting wind integration. *Environ Res Lett* 2013;8. <https://doi.org/10.1088/1748-9326/8/2/024037>.
- [43] Huskova I, Matrosov ES, Harou JJ, Kasprzyk JR, Lambert C. Screening robust water infrastructure investments and their trade-offs under global change: a London example. *Glob Environ Chang* 2016;41:216–27. <https://doi.org/10.1016/j.gloenvcha.2016.10.007>.
- [44] Reed PM, Hadka D, Herman JD, Kasprzyk JR, Kollat JB. Evolutionary multi-objective optimization in water resources: the past, present, and future. *Adv Water Resour* 2013;51:438–56. <https://doi.org/10.1016/j.advwatres.2012.01.005>.
- [45] Deb K, Pratap A, Agarwal S, Meyarivan T. A fast and elitist multiobjective genetic algorithm: NSGA-II. *IEEE Trans Evol Comput* 2002;6:182–97. <https://doi.org/10.1109/4235.996017>.
- [46] Hadka D, Reed P. Diagnostic assessment of search controls and failure modes in many-objective evolutionary optimization. *Evol Comput* 2012;20:423–52. https://doi.org/10.1162/EVCO_a.00053.
- [47] Inselberg A. Multidimensional detective. *Proc VIZ '97 Vis conf inf vis symp parallel render symp*, IEEE comput soc 1997. p. 100–7. <https://doi.org/10.1109/INFVIS.1997.636793>.
- [48] Zitzler E, Thiele L, Laumanns M, Fonseca CM, Da Fonseca VG. Performance assessment of multiobjective optimizers: an analysis and review. *IEEE Trans Evol Comput* 2003;7:117–32. <https://doi.org/10.1109/TEVC.2003.810758>.

- [49] Kasprzyk JR, Reed PM, Characklis GW, Kirsch BR. Many-objective de Novo water supply portfolio planning under deep uncertainty. *Environ Model Softw* 2012;34:87–104. <https://doi.org/10.1016/j.envsoft.2011.04.003>.
- [50] Fleming Peter J, Purshouse Robin C, Lygoe Robert J. Many-Objective Optimization: An Engineering Design Perspective. *EMO: International Conference on Evolutionary Multi-Criterion Optimization* 2005. https://doi.org/10.1007/978-3-540-31880-4_2.
- [51] Woodruff Matthew J, Reed Patrick M, Simpson Timothy W. Many objective visual analytics: rethinking the design of complex engineered systems. *Struct Multidiscip O* 2013. <https://doi.org/10.1007/s00158-013-0891-z>.
- [52] Teytaud Oliver. On the Hardness of Offline Multi-objective Optimization. *Evol Comput* 2007;15(4):475–91. <https://doi.org/10.1162/evco.2007.15.4.475>.